Journal of Clinical and Translational Hepatology **2022**
DOI: 10.14218/JCTH.2022.00128

Original Article

Hepatic Alarmins and Mitochondrial Dysfunction under Residual Hyperlipidemic Stress Lead to Irreversible NAFLD

Luminita Ivan[1], Elena Uyy[1], Viorel I. Suica[1], Raluca M. Boteanu[1], Aurel Cerveanu-Hogas[1], Rune Hansen[2,3] and Felicia Antohe[1*]

[1]Department of Proteomics, Institute of Cellular Biology and Pathology "Nicolae Simionescu" of the Romanian Academy, Bucharest, Romania; [2]Department of Health Research, SINTEF Digital, Trondheim, Norway; [3]Department of Circulation and Medical Imaging, Norwegian University of Science and Technology, Trondheim, Norway

Received: 16 March 2022 | **Revised:** 6 June 2022 | **Accepted:** 12 June 2022 | **Published:** 14 July 2022

Abstract

Background and Aims: Nonalcoholic fatty liver disease (NAFLD) includes a range of progressive disorders generated by excess lipid accumulation in the liver leading to hepatic steatosis and eventually fibrosis. We aimed to identify by high performance mass spectrometry-based proteomics the main signaling pathways and liver proteome changes induced by hypercholesterolemia in a rabbit atherosclerotic model that induced high accumulation of lipids in the liver. ***Methods:*** The effect of combined lipid-lowering drugs (statins and anti-PCSK9 monoclonal antibody) were used after the interruption of the hypercholesterolemic diet to identify also the potential mediators, such as alarmins, responsible for the irreversible NAFLD build up under the hyperlipidemic sustained stress. ***Results:*** Proteomic analysis revealed a number of proteins whose abundance was altered. They were components of metabolic pathways including fatty-acid degradation, glycolysis/gluconeogenesis, and nonalcoholic fatty liver disease. Mitochondrial dysfunction indicated alteration at the mitochondrial respiratory chain level and down-regulation of NADH: ubiquinone oxidoreductase. The expression of a majority of cytochromes (P4502E1, b5, and c) were up-regulated by lipid-lowering treatment. Long-term hyperlipidemic stress, even with a low-fat diet and lipid-lowering treatment, was accompanied by alarmin release (annexins, galectins, HSPs, HMGB1, S100 proteins, calreticulin, and fibronectin) that generated local inflammation and induced liver steatosis and aggressive fibrosis (by high abundance of galectin 3, fibronectin, and calreticulin). ***Conclusions:*** The novel findings of this study were related to the residual effects of hyperlipidemic stress with consistent, combined lipid-lowering treatment with statin and inhibitor of PCSK9.

Citation of this article: Ivan L, Uyy E, Suica VI, Boteanu RM, Cerveanu-Hogas A, Hansen R, *et al*. Hepatic Alarmins and Mitochondrial Dysfunction under Residual Hyperlipidemic Stress Lead to Irreversible NAFLD. J Clin Transl Hepatol 2022. doi: 10.14218/JCTH.2022.00128.

Introduction

Nonalcoholic fatty liver disease (NAFLD) is a metabolic liver disease often associated with obesity that is characterized by fatty infiltration (steatosis) of the liver in the absence of chronic alcohol consumption. NAFLD is based on different liver disorders characterized by accumulation of fat in more than 5% of hepatocytes, primarily in the form of triacylglycerols, resulting from alteration of the homeostatic mechanisms that regulate synthesis of fat in the liver.[1] The consensus of a recent panel of international experts proposed that the name NAFLD be changed to metabolic-associated fatty liver disease (MAFLD).[2,3] It is closely related to metabolic syndrome, and has a common pathophysiology and complex vascular dysfunctions associated with severe cardiovascular diseases (CVDs) including atherosclerosis. There is general agreement that liver inflammation is associated with an accumulation of inflammatory leukocytes and an increase in hepatic and extrahepatic cytokine production. The inflammation might be present in the liver intermittently and/or in a chronic-relapsing manner that may also explain why liver fibrosis can have a role in CVD development.[4]

Therapies aiming to reduce the levels of circulating low-density lipoprotein-cholesterol (LDL-C) decrease the risk of cardiovascular disease at all levels of prevention. Statins,

Keywords: Nonalcoholic fatty liver disease; Atherosclerosis; Proteomic; Alarmins; Fibrosis.

Abbreviations: ACAD10, acyl-CoA dehydrogenase family member 10; ACADS, acyl-CoA dehydrogenase short-chain; ACSL5, acyl-CoA synthetase long-chain family member 5; ACSS2, propionate Co A ligase; ADH2-2, alcohol dehydrogenase class-2 isozyme 2; ALDH7A1, aldehyde dehydrogenase NAD+7 family A1; ALDOB, fructose-biphosphate aldolase B; ANXA1, annexin A1; ANXA3, annexin A3; ANXA4, annexin A4; ANXA5, annexin A5; ANXA6, annexin A6; ANXA11, annexin A11; ANXA13, annexin A13; CALR, calreticulin; CVD, cardiovascular disease; CYB5A, cytochrome b5; CYCS, cytochrome c; CYP2E1, cytochrome P4502E1; DAMP, damage-associated molecular pattern; FN1, fibronectin; HBGB1, high-mobility-group-box 1; HSP70A2, heat shock protein family A (Hsp70) member 2; HSP70A4, heat shock protein family A (Hsp70) member 4; HSP70A5, 78 kDa glucose-regulated protein; HSP90B1, endoplasmin; LDHD, lactate dehydrogenase; LDL-C, low-density lipoprotein-cholesterol; LDLR, low-density lipoprotein receptor; LGALS1, galectin 1; LGALS2, galectin 2; LGALS3, galectin-3; NAFLD, nonalcoholic fatty liver disease; NDUFA6, NADH: ubiquinone oxidoreductase subunit A6; NDUFA9, NADH: ubiquinone oxidoreductase subunit A9; NDUFS1, NADH: ubiquinone oxidoreductase 75 kDa subunit 1; NDUFS3, NADH dehydrogenase [ubiquinone] iron-sulfur protein 3; NDUFS6, NADH dehydrogenase [ubiquinone] iron-sulfur protein 6; PCK1, phosphoenolypyruvate carboxykinase; PCSK9, proprotein convertase subtilisin kexin type 9; PDHB, pyruvate dehydrogenase E1 component subunit beta; PKLR, pyruvate kinase; ROS, reactive oxygen species; UQCR, cytochrome b-c1 complex.

[*]**Correspondence to:** Felicia Antohe, Institute of Cellular Biology and Pathology "N. Simionescu" 8, B.P. Hasdeu Street, PO Box 35-14, Bucharest 050568, Romania. ORCID: https://orcid.org/0000-0002-3325-2867. Tel: +40-21-3194518, Fax: +40-21-3194519, E-mail: felicia.antohe@icbp.ro

drugs that block the activity of the enzyme 3-hydroxy-3-methylglutaryl Coenzyme A reductase, which is linked with the first step of cholesterol biosynthesis, are the main treatment for hyperlipidemia.[5] Inhibitors of proprotein convertase subtilisin kexin type 9 (PCSK9) are a new therapeutic approach to further reduce the levels of LDL-C. Decreased synthesis of PCSK9 or blockage of its association with low-density lipoprotein receptor (LDLR) represent a viable alternative to traditional therapies. Reduced binding of PCSK9 to LDLR restores the normal cycling of the receptors and internalization of LDL-C, leading to reduced progression of atherosclerotic plaques.

PCSK9 is mainly expressed by hepatocytes, and as the most effective mediator of the LDL receptor degradation, is the main regulator of LDL-C homeostasis. PCSK9 binds to the LDL receptor and is internalized as a PCSK9-LDLR complex, which delivers LDLR to lysosomes for degradation. Increased binding activity of PCSK9 leads to hypercholesterolemia, reflecting the increased removal of receptors from the plasma membrane, and resulting in failure to bind and clear LDL-C from plasma.[6] Excess circulating cholesterol is also removed by other nonspecific mechanisms, such as scavenger receptors, and other lipoproteins leading to lipid accumulation in the liver that, in the long term, generate NAFLD. The accumulated lipids cannot be efficiently metabolized because loaded hepatocytes become dysfunctional. Fatty-acid metabolism is altered, and mitochondrial energy production become insufficient for the cell's metabolic homeostatic coordination.[7,8] Mitochondrial dysfunction is reported to be associated with NAFLD and to play a critical role in the pathogenesis of the disease.[9] In addition, lipid deposits that form in the arterial vasculature lead to the constant and slow development of atherosclerotic plaques driven by a failure to resolve the inflammatory response in the arterial wall initiated by the retention of LDL particles. Anti-PCSK9 antibodies that efficiently disrupt the PCSK9-LDLR interaction have been developed. Evolucumab, a human IgG antibody that binds to PCSK9 in a 1 to 1 ratio, is currently used in the clinic. After binding to PCSK9, the antibody impairs the association of PCSK9 with LDLR. In the absence of PCSK9, the receptor is transported back to the plasma membrane, ready to pick up additional LDL particles.[10]

Although the association of NAFLD with hyperlipidemia is well described, it is not yet known whether it actively contributes to, or is only a passenger in the pathogenesis of atherosclerosis. In this study we used high performance mass spectrometry-based proteomics and an accepted rabbit atherosclerosis model[11] to identify the main signaling pathways and liver proteome changes induced by hypercholesterolemia that resulted in the high accumulation of lipids in the liver. After the interruption of the hypercholesterolemic diet, the effects of combined lipid-lowering drugs (statins and anti-PCSK9 antibodies) were used to identify potential mediators, such as alarmins, responsible for the irreversible NAFLD build up under sustained hyperlipidemic stress. Previously published data from our team describe the function of alarmins, endogenous proteins leading to a rapid sterile inflammatory response upon the release, that maintain and amplify local inflammation in atherosclerosis.[12] The passive release of alarmins has been described in lipid-laden, damaged, apoptotic, necroptotic, or necrotic hepatocytes,[13] but the impact of alarmins on fatty liver disease during treatment of hypolipidemia is not well understood.

Methods

All chemicals used for liquid chromatography (LC) and mass spectrometry (MS) experiments were of LC-MS grade. Trypsin Gold was purchased from Promega (Madison, WI, USA). Urea, sodium deoxycholate (DOC), Trizma hydrochloride (Tris), DL-dithiothreitol (DTT), iodoacetamide (IAA), N-acetyl-L-cysteine (NAC), ethylenediaminetetraacetic acid (EDTA), bovine serum albumin (BSA), and all solvents were provided by Sigma Aldrich, unless otherwise specified. Complete protease inhibitor cocktail was from Roche (Mannheim, Germany). C18 solid phase extraction columns were acquired from Waters Corporation (Milford, CT, USA). Protein concentration was determined with bicinchoninic BCA assay kits (Thermo Fisher Scientific, Inc., Rockford, IL61101, USA). Plasma cholesterol, glucose, and triglyceride levels were determined using specific assay kits from DIALAB GMBH, England. Evolocumab, a monoclonal antibody against PCSK9, was purchased from Amgen Europe B.V. (Breda, Netherlands).

Experimental animal model

Twenty-one New Zealand White rabbits were randomly divided into three groups of seven animals each. The control group (C) received standard food for 12 weeks. The atherosclerotic group (A) received hypercholesterolemic diet for the first 8 weeks and standard food for the following 4 weeks. The treated atherosclerotic (At) group received a hypercholesterolemic diet in the first 8 weeks and standard food combined with lipid-lowering drugs for the next 4 weeks. The weekly treatment contained anti PCSK9 antibody (evolocumab, subcutaneous, 25 mg/kg body weight) and daily gavage administration of atorvastatin (3 mg/kg body weight). The animals received 100 g/animal/day of the standard or hypercholesterolemia diet prepared by adding 0.5% cholesterol and 5% corn oil. At the end of the intervention, auricular ear blood was collected from each animal in coagulation-promoting tubes and centrifuged at 1,500×*g* for 15 min at 4°C to obtain the serum, further stored at −80°C for biochemical analysis. The animals were euthanized by intravenous injection of a mixture of ketamine-xylazine (1:1.1 mg/kg body weight) and immediately after abdominal opening, a sample (500 mg) of the left liver lobe was harvested from each animal and rapidly frozen in liquid nitrogen until biochemical assays and MS were performed.

All experimental protocols were approved by the Ethic Committee of Institute of Cellular Biology and Pathology "Nicolae Simionescu" and by the National Sanitary Veterinary and Food Safety Authority (No. 365/12.07.2017) in accordance with Directive 2010/63 of European Union.

Histological study

Liver samples were fixed in 4% (w/v) paraformaldehyde solution, embedded in paraffin, and 6 μm serial sections were double-stained with hematoxylin and eosin (HE) using fast staining kits (Carl Roth GmbH and Co. KG-Karlsruhe, Germany) to show the histological structure following the experimental procedures. Collagen was stained with Masson's trichrome (Carl Roth GmbH + Co. KG-Karlsruhe, Germany). Tissue sections were mounted with Neo-Mount (Merck KGaA, Darmstadt, Germany) and examined with an Axio-Vert A1 inverted microscope (Carl Zeiss GmbH, Göttingen, Germany) and analyzed with Zen Pro 2012 Software (Carl Zeiss GmbH, Göttingen, Germany).

Protein extraction

Thirty milligrams of liver samples were mechanically homogenized (1 min) on ice in 0.3 mL buffer containing 8 M

urea, 1% DOC and 100 mM Tris-HCl (pH 7.5), and centrifuged at 11,000×*g* at 4°C for 10 min. The supernatants were collected and stored at −30°C until use. Protein concentration was determined with a BCA assay kit (Thermo Scientific). The protein extracts were subsequently used for MS and western blotting.

Liver tissue sample preparation for mass spectrometric analysis

After solubilization, 50 μg of the proteins from each sample (three replicates) was purified by acetone precipitation and incubated for 60 min at −20°C. The cysteine residues were processed in a reducing buffer containing 8 M urea, 0.1 M Tris-HCl, 0.1 mol/L EDTA and 20 mmol/L DTT, pH 8.8 for 60 min, followed by alkylation with 80 mmol/L IAA in 0.1 M Tris-HCl and 0.1 mmol/L EDTA buffer, for 90 min in the dark with constant agitation (600 rpm) at room temperature. Quenching was done with 80 mmol/L NAC in 0.1 M Tris-HCl and 0.1 mmol/L EDTA buffer and shaking for 30 min at room temperature. Proteolysis was performed overnight, at 37°C, using a 1: 20 trypsin: substrate quantity ratio. Formic acid was added to the resulting peptide mixtures up to pH 2.5 for enzyme inhibition and DOC precipitation. The sedimented ionic detergent was discarded after centrifugation for 20 min at 20,000×*g* at room temperature. The peptides were desalted by solid phase extraction and concentrated (Concentrator plus; Eppendorf AG, Hamburg, Germany).

Liquid chromatography-tandem mass spectrometric (LC-MS/MS) analysis

The experiments were carried out using the EASY n-LC II system coupled to an LTQ Orbitrap Velos Pro mass spectrometer (both Thermo Fisher Scientific). For chromatographic separation, a trap column (EASY column, 2 cm length × 100 μm inner diameter, 5 μm particle size, 120 Å pore size, Thermo Scientific) was connected to the analytical column (EASY column, 10 cm × 75 μm.d., C18, 3 μm,120 Å, Thermo Scientific). The samples were injected in triplicate, with the same amount of peptide mixture (1 μg) separated and eluted using a 90 min 3–25 % solvent B (99.9 % acetonitrile and 0.1 % formic acid) over solvent A (99.9 % water and 0.1 % formic acid) gradient, at 300 nL/min. The MS was operated in top 15 data-dependent acquisition. Proteome Discoverer 2.4 (Thermo Scientific) and Sequest HT were used for protein inference in UniProtKB/SwissProt fasta database. Variable (methionine oxidation, asparagine, and glutamine deamidation) and fixed (cysteine carbamidomethylation) modifications were taken into account. The peptide false discovery rate was set below 0.05. Label-free relative quantification analysis was performed with Proteome Discoverer 2.4 using the Minora Feature Detector node in the processing workflow and the Feature Mapper together with the Precursor Ions Quantifier node in the consensus workflow. The set parameters for the later quantification node were: 90% of replicate features, normalization on the total peptide amount, scaling on controls, average, and analysis of variance hypothesis testing. A spectral abundance alteration of at least 1.5-fold over the control group corroborated with a p-value <0.05 was considered a significant protein level variation. The size of the data set was extended using sample permutation for each group. To detect and visualize the possible interaction networks of differentially abundant proteins, we used Search Tool for the Retrieval of Interacting Genes (STRING v11.5) freeware.

Western blot assay

Equal amounts of protein (40 μg/lane) from the liver of the control, A and At groups were separated by 10% sodium dodecyl sulfate polyacrylamide gel electrophoresis (SDS-PAGE) and transferred to nitrocellulose membranes (Bio-Rad Laboratories, Inc., Hercules, CA, USA). Immunodetection was performed using specific primary antibodies against cytochrome c (cat. no. 11940; Cell Signaling Technology; Danvers, MA, USA) and calreticulin (cat. no. PA3-900; Invitrogen, Waltham, MA, USA), diluted 1:1,000 in TBS with 1% BSA followed by the appropriate horseradish peroxidase (HRP)-conjugated secondary antibody (diluted 1:3,000 in TBS with 1% BSA). The immune complexes were detected by enhanced chemiluminescence with ECL Western Blotting Substrate (Thermo Fisher Scientific, Inc.). To normalize target protein level, the total protein staining with Ponceau S after transfer was used.

Gene expression analysis

Total RNA was extracted from the liver tissue using RNeasy Mini Kits (QIAGEN, Hilden, Germany). Nucleic acid quality was assessed with an Agilent 2100 Bioanalyzer (Agilent Technologies, Santa Clara, CA) and quantified with a NanoDrop ND 1000 spectrophotometer (Thermo Scientific). cDNA was generated from 1 μg total RNA with Transcriptor First Strand cDNA Synthesis kits (Roche, Mannheim, Germany). LightCycler 480 SYBR Green I Master mix was used to perform quantitative real-time polymerase chain reaction (qPCR) with a LightCycler System (Roche). All reactions were performed in triplicate, and product specificity was validated by melting-curve analysis. Amplification of the housekeeping gene β-Actin was used for normalization. The primer sequences used were calreticulin forward 5′-AAGGAGCAGTTTCTGGACGG-3′ and reverse 5′-GAACTTGCCCGAACTGAGGA-3′; fibronectin forward 5′-GGCTACCATCACTGGTCTGG-3′ and reverse 5′-GGAAGGGTTACCAGTTGGGG-3′; beta-actin forward 5′-GTGCTTCTAGGCGGACTGTT-3′ and reverse 5′- CGGCCACATTGCAGAACTTT-3′. Relative quantification of gene expression was performed with LightCycler 480 software and the efficiency method.

In vitro cell culture

Hep-G2 human hepatocyte cells (American Type Culture Collection, Manassas, VA, USA) were seeded (1×10^5 cells/mL) and cultivated for 48 h in Dulbecco's modified Eagle medium supplemented with 0.5% serum harvested from the control (C), atherosclerotic (A), and treated atherosclerotic (At) rabbits at 37°C in a 5% CO_2 atmosphere. Total protein was extracted as described for hepatic tissue samples and analyzed by MS. Assays were performed in triplicate.

Statistics

Experimental data derived from at least three independent experiments were reported as mean±standard deviation (SD). Analysis of variance hypothesis was applied for the mass spectrometric analysis and Student t-tests were used to compare the results of western blotting, qPCR, and serum biochemistry assays (cholesterol, LDL, triglycerides, and glucose). For MS bioinformatics analysis, statistical algorithms (Benjamini-Hochberg procedure) were used to correct the p-values based on the false discovery rate (FDR). The statistical analysis was with the Student t-test

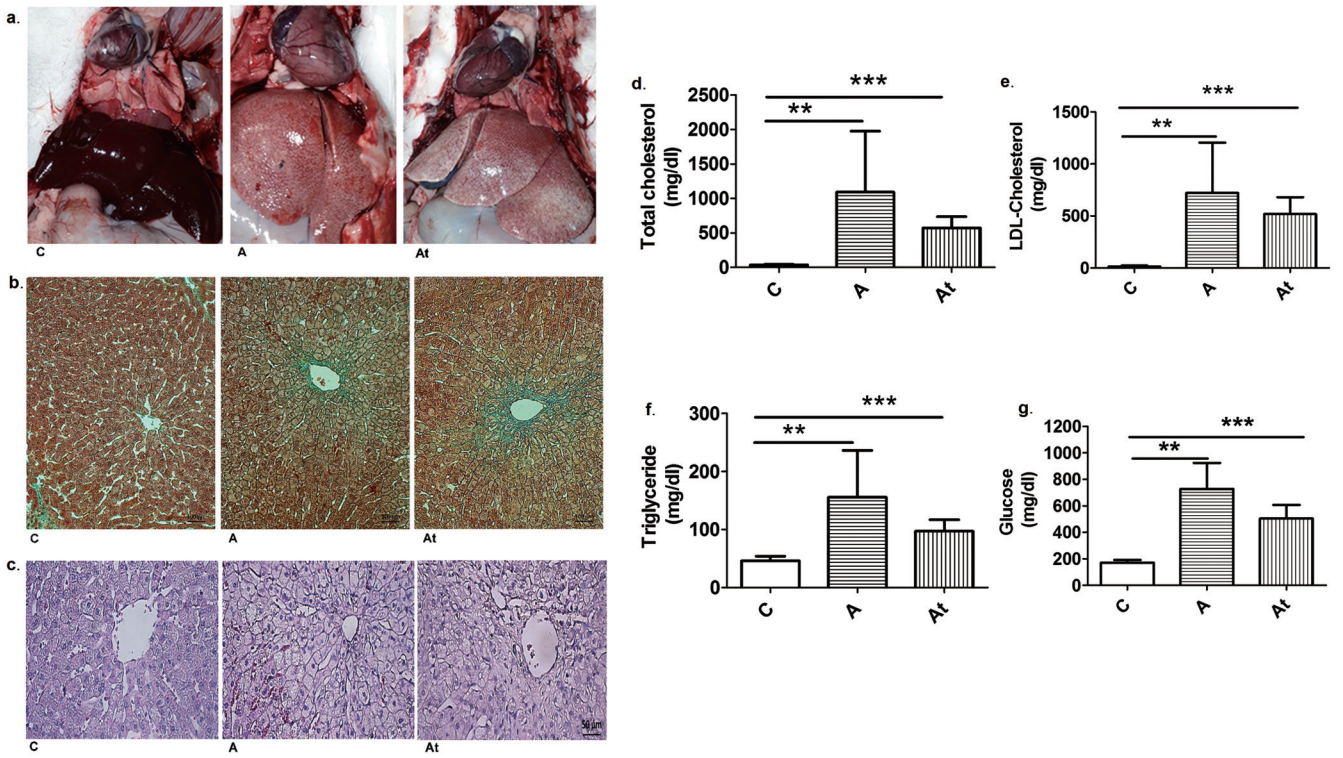

Fig. 1. Lipid accumulation in liver and serum. (a) Macroscopic appearance of hepatic tissue of the control group (C) and hyperlipidemic animals treated with statins and anti PCSK9 antibody (At) or not treated (A). (b) Representative Masson's trichrome stained sections of rabbit liver from the control (C), untreated (A), and treated (At) groups. Nuclei are stained dark red/purple, cytoplasm is stained red/pink, and connective tissue is stained blue. Objective ×20. (c) Original hematoxylin-eosin (HE) stained images of liver sections. Objective ×40. Biochemical lipid and glucose assays in sera from the three study groups at 12 weeks are total cholesterol (d), LDL-cholesterol (e), triglycerides (f) and glucose (g). Serum levels of all animal groups included in the study are shown. Assay results are mean±standard deviation (SD) from seven biological replicates. Statistical evaluation was carried out using the Student *t*-test for unpaired samples. $^{**}p<0.01$; $^{***}p<0.001$.

for unpaired samples and was performed with Prism (version 5, GraphPad Software Inc., La Jolla, CA, USA). Data were reported as mean±SD.

Results

Hepatic lipid accumulation

After 8 weeks of a hypercholesterolemic diet and 4 weeks of standard food, the macroscopic aspect of the liver in the two experimental conditions (treated vs. not treated with statins and inhibitor of PCSK9) showed a heavy fat loading, with appearance of steatosis in the A and At groups compared with the group C. The physical properties of the fatty hepatic tissue were also changed, becoming friable and prone to rupture. Transfer to a standard diet and administration of lipid-lowering drugs induced a small degree of liver recovery (A vs. At, Fig. 1a). Liver sections from groups A and At (Fig. 1b, c) show that hepatocytes near the central vein were more rounded and larger than cells from the control group. The livers of rabbits that received the hyperlipidemic diet had early steatosis with abundant lipid droplets and severe alterations, such as ballooning degeneration, Mallory Denk bodies, and hepatocytes with lost nuclei. Masson trichrome staining was used to assess the degree of liver fibrosis.

The hyperlipidemic diet induced a significant increase of serum lipid parameters (total cholesterol, LDL-cholesterol and triglycerides) in the A and At groups compared with the healthy animals in group C. Total cholesterol was 31.6-fold higher ($p\leq0.01$) in group A and 16.6-fold higher ($p\leq0.001$) in group At versus the control group (Fig. 1d). Moreover, the LDL-cholesterol was increased 56.2-fold in group A ($p\leq0.01$) and 40.4-fold in group At ($p\leq0.001$) compared with serum levels in the group C (Fig. 1e). Serum triglycerides were 3.4-fold higher ($p\leq0.01$) in group A and 2.1 fold higher ($p\leq0.001$) in At compared with group C (Fig. 1f). The hyperlipidemic diet also induced a significant increase of serum glucose in A and At compared with the healthy animals in C. Serum glucose was 4.2-fold higher ($p\leq0.01$) in group A and 2.9-fold higher ($p\leq0.001$) in group At versus the group C (Fig. 1g).

The switch to a standard diet after 2 months and starting lipid-lowering treatment in the At group induced an moderate decrease in total cholesterol by 1.9-fold, LDL-cholesterol by about 1.4-fold, triglycerides by 1.6-fold and glucose by 1.4-fold compared with the A group (Fig. 1d–g), showing that there were improvements in the biochemical parameters evaluated during disease evolution (At versus A). However, the hyperlipidemic diet including 0.5% cholesterol and 5% corn oil administered to rabbits for at least 2 months induced massive accumulation of lipids in the liver leading to steatosis and subsequent development of NAFLD.

LC-MS/MS proteomic analysis

Liver homogenate protein extracts (20 µg/ml in triplicate) and human cell culture-loaded hepatocytes from the three experimental groups were analyzed by tandem MS. Bioinformatics analysis evidenced with good confidence that 1,285 proteins in liver and 981 in hepatocytes were dif-

Table 1. KEGG Pathways significantly altered in fatty liver tissue and cell culture lipid-loaded human hepatocytes

Name of pathway	KEGG description	Count in network	False discovery rate
ocu00071	Fatty-acid degradation	6 of 36	10.6 e^{-03}
hsa00071	Fatty-acid degradation	15 of 42	3.96 e^{-08}
ocu00010	Glycolysis/gluconeogenesis	13 of 51	8.76 e^{-07}
hsa00010	Glycolysis/Gluconeogenesis	13 of 65	9.56 e^{-05}
ocu04932	Nonalcoholic fatty liver disease	11 of 122	8.7 e^{-04}
hsa04932	Nonalcoholic fatty liver disease	18 of 148	6.3 e^{-04}

ferentially altered by 1.5-fold by persistent hyperlipidemic stress. Significantly down or up-regulated proteins (<0.67-fold and >1.5-fold, $p \leq 0.05$) induced by hyperlipidemia in the presence or absence of low-fat therapy were correlated with various signaling pathways identified in the Kyoto Encyclopedia of Genes and Genomes (KEGG) database using the STRING program (v 11.5). The statistically significant pathways in fatty liver disease were selected and are shown in Table 1. The MS results of proteome changes obtained from lipid-loaded hepatocytes in cell culture are shown in Supplementary Table 1 and corroborate very well with the effects of hyperlipidemic stress in the liver tissue.

Fatty-acid degradation pathway

Proteomic analysis revealed five proteins involved in fatty-acid degradation that were significantly deregulated, contributing to the impairment of lipid homeostasis. Histograms in Figure 2b–f shows that the enzymes alcohol dehydrogenase class-2 isozyme 2 (ADH2-2), aldehyde dehydrogenase NAD+7 family A1 (ALDH7A1), acyl-CoA dehydrogenase family member 10 (ACAD10), acyl-CoA dehydrogenase short-chain (ACADS), and acyl-CoA synthetase long-chain family member 5 (ACSL5) decreased significantly in group A compared with group C. Also, ALDH7A1, ACAD10, ACADS, and ACSL5 decreased significantly in At group compared with group C. Three of the five enzymes (ADH2-2, ACAD10, and ACADS, representing 60% of the total proteins in the fatty-acid degradation pathway) increased significantly in abundance following lipid-lowering treatment (At vs. A).

Proteomic analysis of fat-loaded hepatocytes in culture (serum from groups A and At) found that 15 proteins altered by hyperlipidemic stress were also involved in the fatty-acid degradation pathway (Supplementary Table 1). Two proteins (ACADS and ALDH7A) were found both in the liver tissue and the hepatocytes from cell cultures.

Glycolysis/gluconeogenesis pathway

Bioinformatics analysis of liver samples revealed another

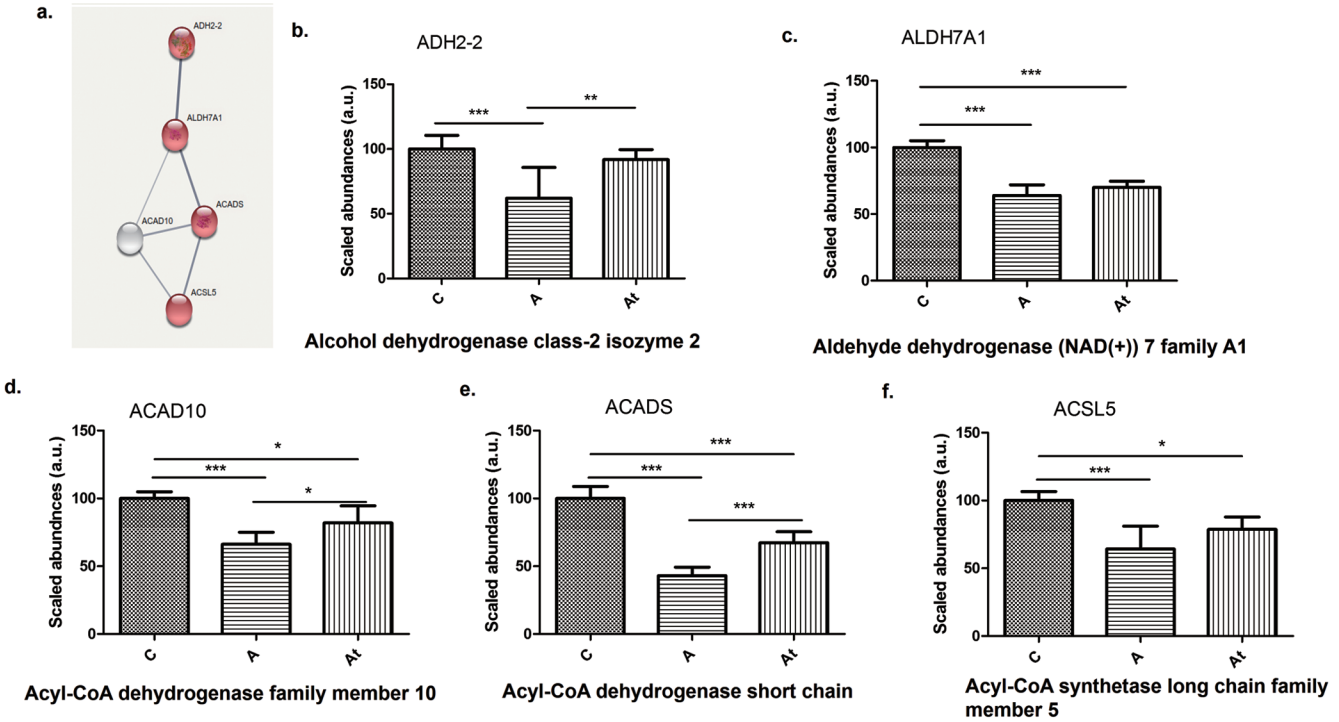

Fig. 2. Protein-protein interaction. (a) Highlighted by STRING v.11.5 analysis. (b–f) Identification and relative quantification of proteins in the fatty-acid degradation pathway in groups C, A, and At. Data are mean±SD of three biological replicates, each with three technical replicates. *p<0.05, **p<0.01, ***p<0.001 versus the control group.

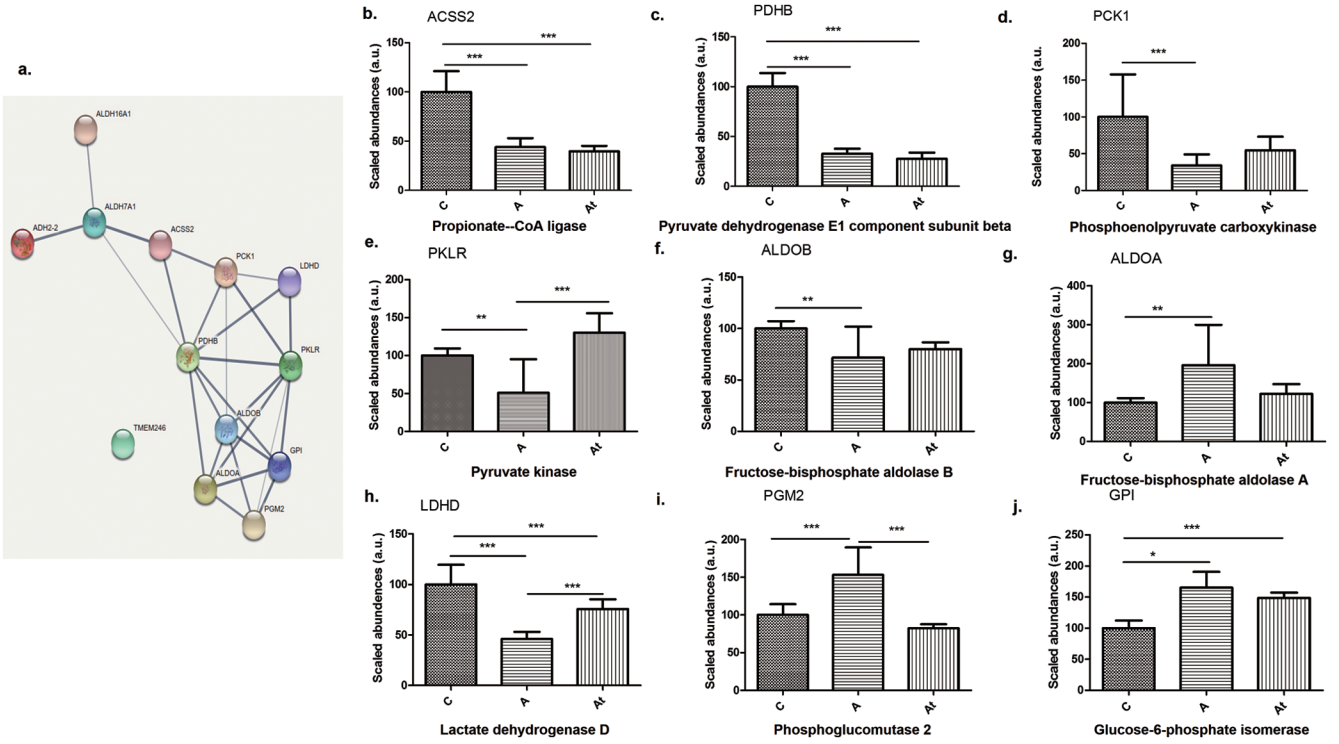

Fig. 3. Differentially abundant proteins. (a) Included in the glycolysis/gluconeogenesis pathway. (b–j) Identification and quantification of proteins in the glycolysis/gluconeogenesis pathway in the three study groups. Data are mean±SD of three biological replicates, each with three technical replicates. *p<0.05, **p<0.01, ***p<0.001 versus the control group.

statistically relevant signaling pathway, glycolysis/gluconeogenesis (FDR=8.76e^{-07}). In this signaling pathway, we found proteins that were also involved in the fatty-acid degradation pathway, such as ADH2-2 and ALDH7A1. In addition, the abundance of most of the identified enzymes (80% of total proteins analyzed) involved in glycolysis/gluconeogenesis pathway were significantly decreased in group A compared with group C, including ADH2-2, ALDH7A1, propionate Co A ligase (ACSS2), pyruvate dehydrogenase E1 component subunit beta (PDHB), phosphoenolypyruvate carboxykinase (PCK1), pyruvate kinase (PKLR), fructose-biphosphate aldolase B (ALDOB), and lactate dehydrogenase (LDHD). The results showed that 30% of the analyzed enzymes significantly increased in abundance after lipid-lowering treatment (At vs. A): ADH2-2 (Fig. 2b), pyruvate kinase (PKLR), and LDHD (Fig. 3e, h). In addition, 13 proteins in lipid-loaded hepatocytes from cell cultures were involved in the same glycolysis/gluconeogenesis pathway. Abundances expressed as A/C and At/C ratios and the significant differences are shown in Supplementary Table 1.

Mitochondrial dysfunction

Interestingly, the proteomic analysis of liver homogenates showed that a number of proteins involved in mitochondrial oxidative phosphorylation were significantly disrupted, which may have contributed to the progression of NAFLD. For example, proteins in the mitochondrial respiratory chain from complex I decreased significantly in the At group, including NADH: ubiquinone oxidoreductase 75 kDa subunit 1 (NDUFS1), NADH dehydrogenase [ubiquinone] iron-sulfur protein 3 (NDUFS3), NADH dehydrogenase [ubiquinone] iron-sulfur protein 6 (NDUFS6), NADH: ubiquinone oxidoreductase subunit A6 (NDUFA6), and NADH: ubiquinone oxidoreductase subunit A9 (NDUFA9) (Fig. 4b–f). After switching to a standard diet after two months and introducing lipid-lowering treatment in the At group, the following proteins from the electron transport chain were found to be significantly less abundant: NDUFS1, NDUFS3, NDUFS6, NDUFA6, and NDUFA9 (Fig. 4b–f).

Remarkably, the MS data revealed that hyperlipidemia induced a significant change in a group of cytochromes known to be markers of cellular damage and are potential damage-associated molecular pattern (DAMP) candidates. Indeed the protein abundance of all cytochromes identified was significantly increased in groups A and At compared with control C, including cytochrome P4502E1 (CYP2E1), cytochrome b5 (CYB5A), and cytochrome c (CYCS) (Fig. 5a–c). The protein CYCS was unambiguously confirmed by western immunoblotting to be 4.3-fold (p≤0.001) higher in group A and 4.7-fold higher (p≤0.01) in group At than in group C (Fig. 5d). Interesting, hypolipidemia treatment associated with the standard diet did not have a statistically significant effect on their abundance (A versus At). Assays in human cells loaded with lipids showed a statistically significant increase of about two-fold in the abundance of CYCS and a significant decrease of about five-fold in CYB5A in groups A and At compared with group C (Fig. 5e, f). In lipid-loaded human hepatocytes, six NADH dehydrogenases, two of them from the beta subcomplex (NDUFB8 and NDUFB4) with increased expression and four (NDUFA7, NDUFA13, NDUFB10, and NDUFV1) with significantly decreased expression were found. The A/C and At/C abundance ratios of the cytochrome c oxidase (COX) and cytochrome b-c1 complex (UQCR) enzymes are shown in Supplementary Table 1.

Taken together, the data support the hypothesis that chronic hyperlipidemia induced severe mitochondrial damage and an oxidative stress pathway that may promote vi-

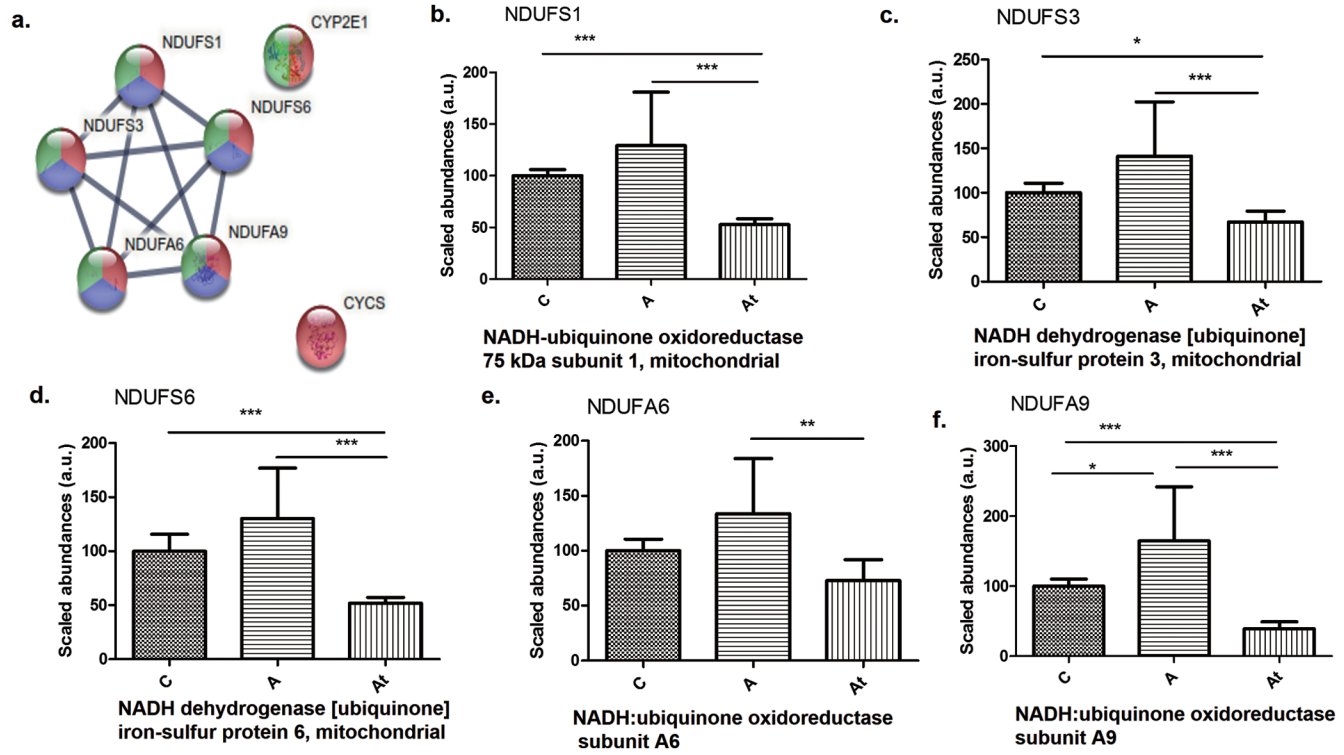

Fig. 4. Protein-protein interaction in the nonalcoholic fatty liver disease pathway. (a) Highlighted by STRING v.11.5 analysis. (b–f) Identification and quantification of proteins in this pathway in the three study groups. Data are mean±SD from three biological replicates, each with three technical replicates. *p<0.05, **p<0.01, ***p<0.001 versus the control group.

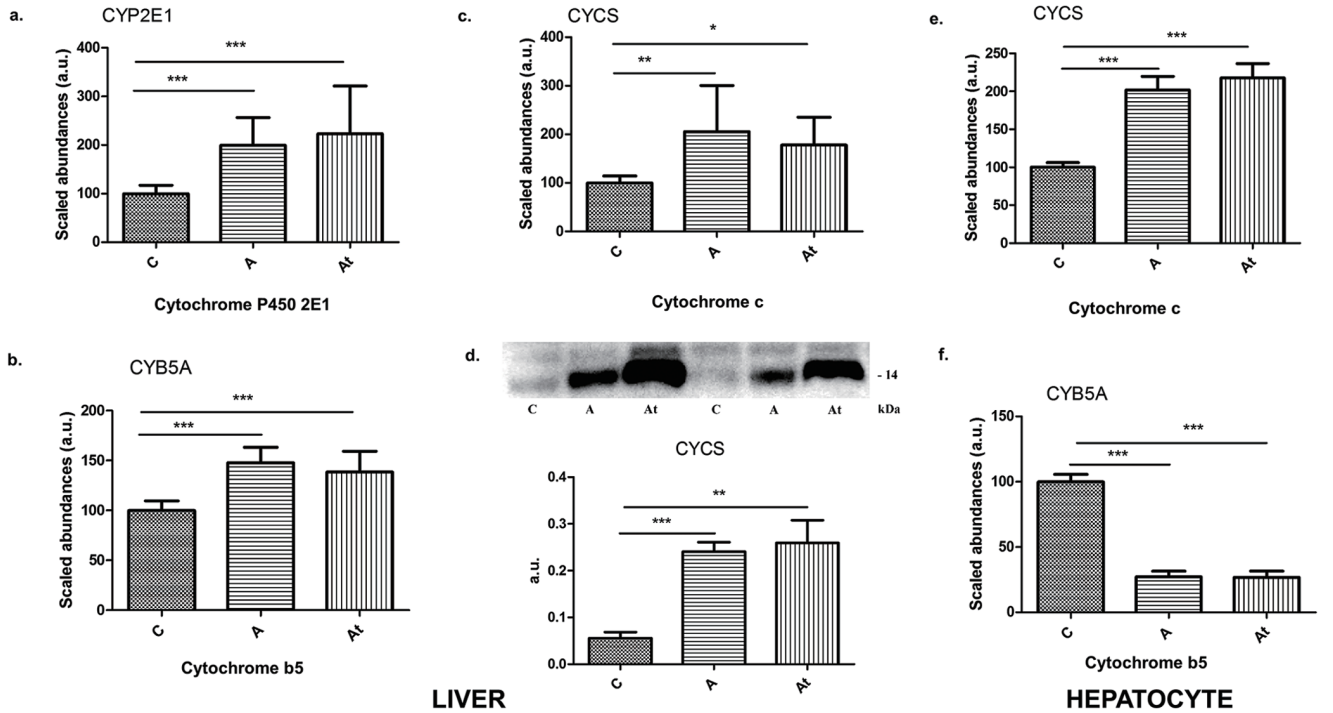

Fig. 5. Identification and quantification of cytochromes. (a–c) CYP2E1 (a), CYB5A (b), and CYCS (c) in the nonalcoholic fatty liver disease pathway in the three study groups. (d) Validation of spectral data for cytochrome c by western blotting densitometry and corresponding histogram (lower panel) for the three experimental groups. (e–f) Identification and quantification of cytochromes CYCS (e) and CYB5A (f) in the nonalcoholic fatty liver disease pathway from human hepatocytes incubated with serum from the three study groups. Data are mean±SD of three biological replicates, each with three technical replicates. *p<0.05, **p<0.01; ***p<0.001 versus the control group.

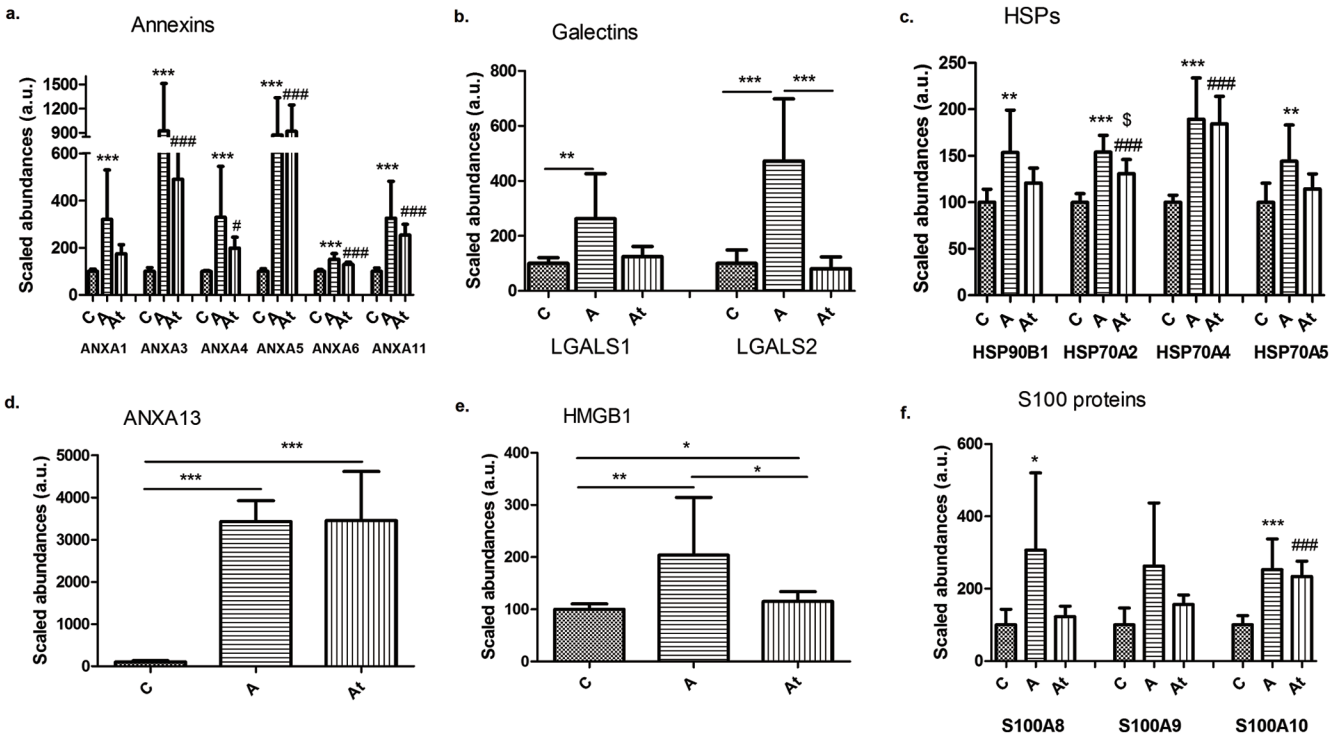

Fig. 6. Identification and quantification of different classes of alarmins. (a–f) Annexins (a, d), galectins (b), HSPs (c), HMGB1 (e) and S100 proteins (f) in the three study groups. Data are mean±SD of three biological replicates, each with three technical replicates. *A/C, #At/C and $A/At; *$p$<0.05, **$p$<0.01, ***$p$<0.001, $$p$<0.05, #$p$<0.05, #$p$<0.001.

tal cytochrome dysfunction or cell death during persistent hyperlipidemia. The novel data presented above clearly indicate measurable changes in the abundance of enzymes involved in the functional pathways of fatty acids degradation, glycolysis/gluconeogenesis and nonalcoholic fatty liver disease in atherosclerosis group A and short-term atherosclerosis treatment group At.

MS identified DAMPS as NAFLD mediators

Proteomic analysis also provided evidence that the abundance of released DAMPs in liver samples as a potential mediator of the relationship between NAFLD and hyperlipidemia-generated atherosclerosis. DAMPs or alarmins classified as annexins, galectins, heat shock proteins, high-mobility-group-box, and S100 proteins were identified and quantified in liver homogenates and in cell culture-loaded hepatocytes.

The hepatic results showed that there were significant increase in the abundance of a majority of annexins (A1, A3, A4, A5, A6, and A11) in groups A and At compared with group C (Fig. 6a). Annexin 3 and annexin 5 were nine-fold (p<0.001) more abundant in A than in control C (Fig. 6a). Annexin 3 was four- to five-fold (p<0.001) more abundant in hepatocytes incubated with serum from groups A and At compared with those incubated with serum from group C (Supplementary Fig. 1a). Remarkably, the abundance of annexin 13 protein in liver samples increased by approximately 34-fold in groups A and At compared with group C (Fig. 6d), pointing out its key effect in hyperlipidemia. Among members of the galectin family, the abundance of galectin 1 (LGALS1) protein increased 2.6 times and that of galectin 2 (LGALS2) increased 4.7 times in group A (Fig. 6b). The abundance of heat shock proteins in class 90 (HSP90B1) and class 70 (HSP70A2, HSP70A4 and HSP70A5) significantly increased in group A and At compared with group C (Fig. 6c and Supplementary Fig. 1b) The hyperlipidemia diet induced a significant increase in the abundance of nuclear HMGB1 and HMGB3 proteins, by approximately two-fold in group A and 1.15-fold in group At. Switching to a standard diet after 2 months and starting lipid-lowering treatment lead to a significant decrease in HMGB1 abundance of about 1.7-fold in the At compared with the A group (Fig. 6e and Supplementary Fig. 1e). S100A8, S100A10, and S100A4 proteins significantly increased in abundance in group A compared with the group C (Fig. 6f and Supplementary Fig. 1c). An interesting observation shown in Fig. 6b, c, and e was that switching to a standard diet after 2 months and beginning a lipid-lowering treatment induced significant changes in the abundance of only some alarmins (LGALS2, HSP70A2 and HMGB1) while others remained at about the same level as in group A, indicating that their abundance was not be regulated only by reduction of the levels of circulating lipids.

Molecular chaperones, such as calreticulin (CALR), which promotes protein folding by decreasing energy barriers that prevent the aggregation of hydrophobic surfaces during protein maturation, increased in abundance by 1.4-fold in group A (p<0.05), rabbits maintained on the hyperlipidemia diet compared with control rabbits (Fig. 7a). The increase in CALR expression was confirmed by western blotting (Fig. 7b) and qPCR (Fig. 7d). In loaded hepatocytes, the abundance of CALR decreased 1.5-fold in group A (p<0.05) compared with group C (Supplementary Fig. 1f).

In addition, a marker of liver fibrosis, fibronectin (FN1), was significantly increased in group A rabbits on a hyperlipidemic diet by 1.5-fold and remained 1.4-fold enhance in the At compared with C (Fig. 7e). qPCR confirmed that the high abundance of fibronectin in hyperlipidemic liver tissue was accompanied by a 45% increase in gene expres-

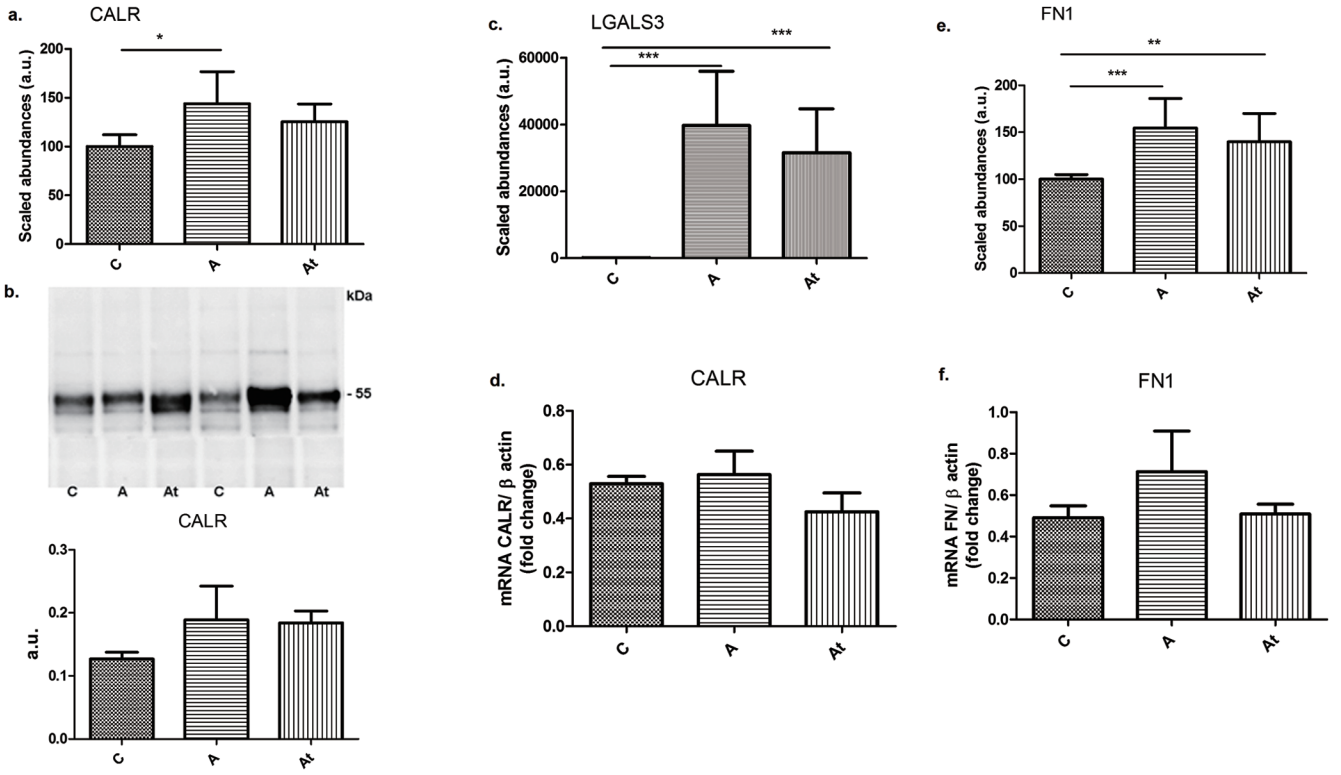

Fig. 7. Mass spectrometry quantitative evaluation of the abundance of three important proteins involved in liver fibrosis. (a, c, e) Calreticulin (CALR) (a), galectin-3 (LGALS3) (c), and fibronectin (FN1) (e). (b, d, f). Validation of mass spectrometry data for calreticulin by western blotting (b) and qPCR (d) and for fibronectin by qPCR (f). Data are mean±SD of three biological replicates, each with three technical replicates. *p<0.05, **p<0.01, ***p<0.001.

sion in group A (Fig. 7f). Published data[14,15] indicates that FN is associated with cell cycle progression, participates in cell adhesion and proliferation, and has an important role in fibrosis progression together with another protein, galectin-3 (LGALS3).[16] MS relative quantification demonstrated a significant 397-fold increase in protein expression in group A and a 315-fold increase in group At relative to control probes (Fig. 7c) and an approximately two-fold increase in cells incubated with serum from groups A or At (Supplementary Fig. 1d). The *in vivo* and in cell culture results clearly show that persistent hyperlipidemic stress was accompanied by high expression of proteins involved in liver fibrogenesis.

Discussion

NAFLD includes a range of progressive disorders generated by excess lipid accumulation in the liver leading to hepatic steatosis and eventually to fibrosis, cirrhosis, and hepatocellular carcinoma.[17] NAFLD has a strong association with CVD risk factors. As the liver has a central role in lipid and glucose metabolism, it is a basic component of cardio-metabolic diseases, such as diabetes mellitus and metabolic syndrome. The mechanism of the relationship between NAFLD and hyperlipidemic vascular diseases is not fully understood, especially under a lipid-lowering treatment combined with a low-fat diet.

Published studies describe NAFLD as closely associated with atherogenic dyslipidemia, hyperglycemia, and inflammation.[18] However, the described mechanisms and the involved proteins were not completely described or considered. In NAFLD, published data show that hepatic fat accumulation results from an imbalance of lipid acquisition and lipid disposal mediated by inadequate uptake of circulating lipids, increased hepatic de-novo lipogenesis, insufficient enhancement of compensatory fatty-acid oxidation, or altered export of lipids as components of very low-density lipoproteins (VLDL).[19] In this study we took advantage of an in house generated experimental hyperlipidemic animal model in New Zealand White rabbits[20] to search for the liver proteome changes and signaling pathways altered under the hyperlipidemic stress in the presence or absence of lipid-lowering medications.

Histological and biochemical analysis (Fig. 1) of liver sections from the two hyperlipidemic groups (A and At) led to the conclusion that after 8 weeks of a fatty diet, the cells accumulated large deposits of lipids and adipocyte-packed vacuoles similar to those seen in steatosis. The histological hallmark of NAFLD steatosis, is manifested as hepatocellular intracytoplasmic accumulation of lipids, mainly in the form of triglycerides.[21] The experimental animal NAFLD model was similarly characterized by hepatic fatty changes, with lobular hepatitis, focal necrosis containing inflammatory infiltrates, and frequent Mallory bodies and fibrosis as previously described as well.[22] We hypothesized that steatosis hepatocytes induced in NAFLD would undergo not only morphological, but also functional changes. In our study, treating human hepatocytes in culture with hyperlipidemic serum obtained from atherosclerotic rabbits also resulted in the heavy accumulation of lipid droplets in the cells.

Proteomic analysis revealed a number of proteins involved in the metabolic lipids and carbohydrate processes that were significantly altered. The proteins were components of metabolic pathways including fatty acids degradation, glycolysis/gluconeogenesis and NAFLD demonstrating

severe hepatic oxidative stress that resulted in progressive mitochondrial dysfunction and hepatic energy deficit. When one or more of the processes becomes dysregulated, excess lipid accumulation occur. The regulation of fatty-acid partitioning happens at several points, including during triacylglycerol synthesis, lipid droplet formation, and lipolysis.[23]

Indeed, we found that the abundance of some enzymes involved in the three signaling pathways mentioned above were altered by the hypercholesterolemic diet and were not corrected by the lipid-lowering treatment that was administered. Thus, the processes of fatty-acid uptake, fatty-acid synthesis, and the intracellular partitioning of fatty acids into storage, oxidation, and secretion pathways were severely changed, if the lipidic stress was maintained. The statements are supported by the significant differences found in the expression of proteins from complex I – ubiquinone oxidoreductase (NADH) in the experimental groups. The abundance of complex I enzymes (NDUFS1, NDUFS3, NDUFS6, NDUFA6, and NDUFA9) was low in the At group compared with the group C, which indicates mitochondrial membrane damage induced by persistent oxidative stress. NDUFS1 is the target of cleavage by apoptotic caspases contributing to the loss of mitochondrial transmembrane potential, compromised mitochondrial respiration, increased production of mitochondrial reactive oxygen species (ROS), and loss of lysosomal integrity.[24,25] The data corroborate very well with the results of this study that altered lipid metabolism and oxidative stress were implicated in hepatic mitochondrial dysfunction in NAFLD. As expected, the cultured hepatocyte exposed to hyperlipidemic serum become loaded with lipids and showed proteomic changes in NADH dehydrogenase, cytochrome b-c1 complex, cytochrome c oxidase and increased oxidative stress (CYCS) (Supplementary Table 1).

Our results using the experimental hyperlipidemic rabbit model bring new and in-depth evidence of increased oxidative stress[20] that has been reported in patients with NAFLD[26] and atherosclerosis.[27] Patients with NALFD have augmented production of ROS that leads to lipid peroxidation, resulting in inflammation and fibrogenesis through activation of stellate cells. Furthermore, ROS leads to diminished secretion of VLDL and subsequent accumulation of fat in hepatocytes. Excess ROS production is also responsible for oxidation of LDL, which can promote transformation of macrophages to foam cells and is considered to be the first step in the formation of atherosclerotic lesions.[19] As a major site of ROS production, mitochondria are susceptible to oxidative damage. Increased hepatic oxidative stress in NAFLD may stimulate degradation of mitochondrial proteins involved in oxidative defense, and other critical metabolic pathways, including fatty-acid degradation, tricarboxylic acid cycle, and oxidative phosphorylation. The perturbations may result in progressive mitochondrial dysfunction and hepatic energy deficit in NAFLD as shown in this study.

In addition, we found that the abundance of some enzymes involved three signaling pathways (fatty acids degradation, glycolysis/gluconeogenesis, and nonalcoholic fatty liver disease) was modified by the atherosclerotic diet and was mildly ameliorated by short-term lipid-lowering treatment. Bioinformatics analysis disclosed that a multitude of alarmins increased in abundance, highlighted by MS, and pointing out that some of them had a direct link with liver fibrosis. Alarmins can either exert beneficial cell housekeeping functions that lead to tissue repair, or cause deleterious, uncontrolled tissue damage, and persistent local inflammation. As shown here, this group of proteins included HMGB1 and Ca^{2+}-binding S100 proteins.

The fibrosis process is strongly underlined in our study by the excessive abundance of calreticulin, fibronectin, and galectin-3 that was confirmed by immunoblotting and qPCR as well as other methods. The progression of both atherosclerosis and liver fibrosis may be induced by long lasting, persistent, and slowly progressive inflammation induced by oxidative stress and altered lipid metabolic pathways. A combination of oxidative stress, lipid peroxidation, mitochondrial dysfunction, and sustained release of alarmins as inflammatory mediators, leads to progressive irreversible liver injury caused by steatohepatitis and fibrosis that lead to irreversible hepatic damage.

The novel knowledge uncovered by this study is related to the residual effects of hyperlipidemic stress under the consistent combined lipid-lowering treatment with a statin and an inhibitor of PCSK9. (1) Long lasting hyperlipidemic stress is the main risk factor that will induce both progressive development of atherosclerosis and hepatic lipid overload leading to irreversible NAFLD. Foam-cell hepatocytes generated in culture is an additional validation of the stress induced by hyperlipidemia even with adequate medication. (2) The main signaling pathways severely altered by hyperlipidemia were fatty acids degradation, glycolysis/gluconeogenesis and nonalcoholic fatty liver disease. (3) Mitochondrial dysfunction indicated alteration at the mitochondrial respiratory chain level and down-regulation of NADH: ubiquinone oxidoreductase, while expression of the majority of cytochromes (cytochrome P4502E1, cytochrome b5, and cytochrome c) were up-regulated by lipid-lowering treatment. (4) Long-term hyperlipidemic stress even with low-fat diet and lipid-lowering treatment was accompanied by alarmin release (annexins, galectins, HSPs, HMGB1, S100 proteins, calreticulin, and fibronectin) that generated local inflammation and induced liver steatosis and aggressive fibrosis promoted by the high abundance of galectin 3, fibronectin, and calreticulin.

Acknowledgments

We thank Florentina Safciuc, PhD and Gabriela Tanko, PhD for help during experiments with animal model.

Funding

This work was supported by the Romanian Academy and in part by a grant from the Romanian National Authority for Scientific Research and Innovation, CCCDI-UEFISCDI project COFUND-ERA-CVD-XploreCAD, No. 41/2018 within PNCDI III.

Conflict of interest

The authors have no conflict of interests related to this publication.

Author contributions

Study concept and design (FA, LI), acquisition of data (LI, EU, VIS), analysis and interpretation of data (LI, EU, VIS, RB, AHC), drafting of the manuscript (LI, FA), critical revision of the manuscript for important intellectual content (FA, LI, EU, VIS, RH, FA), administrative, technical, or material support (LI, EU, VIS, RB, AHC), and study supervision (FA). All authors have made a significant contribution to this study and have approved the final manuscript.

Ethical statement

All experimental protocols were approved by the Ethic Com-

mittee of Institute of Cellular Biology and Pathology "Nicolae Simionescu" and by the National Sanitary Veterinary and Food Safety Authority (No. 365/12.07.2017) in accordance with Directive 2010/63 of European Union.

Data sharing statement

No additional data are available.

References

[1] Juanola O, Martínez-López S, Francés R, Gómez-Hurtado I. Non-Alcoholic Fatty Liver Disease: Metabolic, Genetic, Epigenetic and Environmental Risk Factors. Int J Environ Res Public Health 2021;18(10):5227. doi:10.3390/ijerph18105227, PMID:34069012.

[2] Xian YX, Weng JP, Xu F. MAFLD vs. NAFLD: shared features and potential changes in epidemiology, pathophysiology, diagnosis, and pharmacotherapy. Chin Med J (Engl) 2020;134(1):8–19. doi:10.1097/CM9.0000000000001263, PMID:33323806.

[3] Heeren J, Scheja L. Metabolic-associated fatty liver disease and lipoprotein metabolism. Mol Metab 2021;50:101238. doi:10.1016/j.molmet.2021.101238, PMID:33892169.

[4] Targher G, Byrne CD, Tilg H. NAFLD and increased risk of cardiovascular disease: clinical associations, pathophysiological mechanisms and pharmacological implications. Gut 2020;69(9):1691–1705. doi:10.1136/gutjnl-2020-320622, PMID:32321858.

[5] Klein-Szanto AJP, Bassi DE. Keep recycling going: New approaches to reduce LDL-C. Biochem Pharmacol 2019;164:336–341. doi:10.1016/j.bcp.2019.04.003, PMID:30953636.

[6] Roth EM, Davidson MH. PCSK9 Inhibitors: Mechanism of Action, Efficacy, and Safety. Rev Cardiovasc Med 2018;19(S1):S31–S46. doi:10.3909/ricm19S1S0002, PMID:30207556.

[7] Qin S, Yin J, Huang K. Free Fatty Acids Increase Intracellular Lipid Accumulation and Oxidative Stress by Modulating PPARα and SREBP-1c in L-02 Cells. Lipids 2016;51(7):797–805. doi:10.1007/s11745-016-4160-y, PMID:27270405.

[8] Vakifahmetoglu-Norberg H, Ouchida AT, Norberg E. The role of mitochondria in metabolism and cell death. Biochem Biophys Res Commun 2017;482(3):426–431. doi:10.1016/j.bbrc.2016.11.088, PMID:28212726.

[9] Prasun P, Ginevic I, Oishi K. Mitochondrial dysfunction in nonalcoholic fatty liver disease and alcohol related liver disease. Transl Gastroenterol Hepatol 2021;6:4. doi:10.21037/tgh-20-125, PMID:33437892.

[10] Chaudhary R, Garg J, Shah N, Sumner A. PCSK9 inhibitors: A new era of lipid lowering therapy. World J Cardiol 2017;9(2):76–91. doi:10.4330/wjc.v9.i2.76, PMID:28289523.

[11] Fan J, Kitajima S, Watanabe T, Xu J, Zhang J, Liu E, *et al*. Rabbit models for the study of human atherosclerosis: from pathophysiological mechanisms to translational medicine. Pharmacol Ther 2015;146:104–119. doi:10.1016/j.pharmthera.2014.09.009, PMID:25277507.

[12] Boteanu RM, Suica VI, Uyy E, Ivan L, Dima SO, Popescu I, *et al*. Alarmins in chronic noncommunicable diseases: Atherosclerosis, diabetes and cancer. J Proteomics 2017;153:21–29. doi:10.1016/j.jprot.2016.11.006, PMID:27840210.

[13] Han H, Desert R, Das S, Song Z, Athavale D, Ge X, *et al*. Danger signals in liver injury and restoration of homeostasis. J Hepatol 2020;73(4):933–951. doi:10.1016/j.jhep.2020.04.033, PMID:32371195.

[14] Matsui S, Takahashi T, Oyanagi Y, Takahashi S, Boku S, Takahashi K, *et al*. Expression, localization and alternative splicing pattern of fibronectin messenger RNA in fibrotic human liver and hepatocellular carcinoma. J Hepatol 1997;27(5):843–853. doi:10.1016/s0168-8278(97)80322-4, PMID:9382972.

[15] Liu XY, Liu RX, Hou F, Cui LJ, Li CY, Chi C, *et al*. Fibronectin expression is critical for liver fibrogenesis in vivo and in vitro. Mol Med Rep 2016;14(4):3669–3675. doi:10.3892/mmr.2016.5673, PMID:27572112.

[16] Li LC, Li J, Gao J. Functions of galectin-3 and its role in fibrotic diseases. J Pharmacol Exp Ther 2014;351(2):336–343. doi:10.1124/jpet.114.218370, PMID:25194021.

[17] Wang J, He W, Tsai PJ, Chen PH, Ye M, Guo J, *et al*. Mutual interaction between endoplasmic reticulum and mitochondria in nonalcoholic fatty liver disease. Lipids Health Dis 2020;19(1):72. doi:10.1186/s12944-020-01210-0, PMID:32284046.

[18] Turan Y. The Nonalcoholic Fatty Liver Disease Fibrosis Score Is Related to Epicardial Fat Thickness and Complexity of Coronary Artery Disease. Angiology 2020;71(1):77–82. doi:10.1177/0003319719844933, PMID:31018673.

[19] Dinani A, Sanyal A. Nonalcoholic fatty liver disease: implications for cardiovascular risk. Cardiovasc Endocrinol 2017;6(2):62–72. doi:10.1097/XCE.0000000000000126, PMID:31646122.

[20] Uyy E, Suica VI, Boteanu RM, Cerveanu-Hogas A, Ivan L, Hansen R, *et al*. Regulated cell death joins in atherosclerotic plaque silent progression. Sci Rep 2022;12(1):2814. doi:10.1038/s41598-022-06762-y, PMID:35181730.

[21] Pan X, Wang P, Luo J, Wang Z, Song Y, Ye J, *et al*. Adipogenic changes of hepatocytes in a high-fat diet-induced fatty liver mice model and non-alcoholic fatty liver disease patients. Endocrine 2015;48(3):834–847. doi:10.1007/s12020-014-0384-x, PMID:25138963.

[22] Lakhani HV, Sharma D, Dodrill MW, Nawab A, Sharma N, Cottrill CL, *et al*. Phenotypic Alteration of Hepatocytes in Non-Alcoholic Fatty Liver Disease. Int J Med Sci 2018;15(14):1591–1599. doi:10.7150/ijms.27953, PMID:30588181.

[23] Hodson L, Gunn PJ. The regulation of hepatic fatty acid synthesis and partitioning: the effect of nutritional state. Nat Rev Endocrinol 2019;15(12):689–700. doi:10.1038/s41574-019-0256-9, PMID:31554932.

[24] Huai J, Vögtle FN, Jöckel L, Li Y, Kiefer T, Ricci JE, *et al*. TNFα-induced lysosomal membrane permeability is downstream of MOMP and triggered by caspase-mediated NDUFS1 cleavage and ROS formation. J Cell Sci 2013;126(Pt 17):4015–4025. doi:10.1242/jcs.129999, PMID:23788428.

[25] Gusdon AM, Song KX, Qu S. Nonalcoholic Fatty liver disease: pathogenesis and therapeutics from a mitochondria-centric perspective. Oxid Med Cell Longev 2014;2014:637027. doi:10.1155/2014/637027, PMID:25371775.

[26] Delli Bovi AP, Marciano F, Mandato C, Siano MA, Savoia M, Vajro P. Oxidative Stress in Non-alcoholic Fatty Liver Disease. An Updated Mini Review. Front Med (Lausanne) 2021;8:595371. doi:10.3389/fmed.2021.595371, PMID:33718398.

[27] Yang X, Li Y, Li Y, Ren X, Zhang X, Hu D, *et al*. Oxidative Stress-Mediated Atherosclerosis: Mechanisms and Therapies. Front Physiol 2017;8:600. doi:10.3389/fphys.2017.00600, PMID:28878685.